Oxidation of Metals, Vol. 25, Nos. 1/2, 1986

Internal Oxidation of Fe–Al Alloys in the α-Phase Region

Jun Takada,* Sadahiro Yamamoto,* Shiomi Kikuchi,* and Masao Adachi*

Received March 25, 1985; revised June 10, 1985

The internal oxidation behavior of Fe-0.069, 0.158, and 0.274 wt% Al alloys was investigated in the α-phase region. The internal oxidation experiments have been made over the temperature range from 1023 to 1123 K using a mixture of iron and its oxide powders. A parabolic rate law holds in the present alloys, where the rate constant, K_p, depends upon the oxidation temperature as well as the aluminum content. The internal oxidation of Fe-Al alloys is, therefore, controlled by a diffusion process of oxygen in the alloy. The oxide formed in the oxidation layer is the stoichiometric $FeAl_2O_4$ (hercynite). The aluminum concentration, N_{Al}^{IO}, in the oxidation layer was calculated by taking account of counterdiffusion of aluminum. Furthermore, the oxygen concentration, N_O^S, at the specimen surface was evaluated on the basis of thermodynamics. Using these estimated values of K_p, N_{Al}^{IO}, and N_O^S, the diffusion coefficient of oxygen, D_O^{IO}, in the oxidation layer, where the oxide particles were dispersed, was also calculated. D_O^{IO} increases as the volume fraction of the oxide, f^{IO}, increases. The diffusion coefficient of oxygen, D_O, in α-iron was determined by extrapolating D_O^{IO} to $f^{IO} = 0$.

KEY WORDS: diffusion coefficient of oxygen; α-iron; internal oxidation; oxygen solubility; counterdiffusion.

INTRODUCTION

Internal oxidation is a preferred oxidation of an alloying element, which is less noble than the solvent metal. Such an oxidation occurs under the

*Department of Metal Science and Technology, Kyoto University, Kyoto 606, Japan. Present address for S. Yamamoto: Technical Research Center, Nippon Kokan K.K., Kawasaki 210, Japan. M. Adachi is Professor Emeritus, Department of Metal Science and Technology, Kyoto University.

0030-770X/86/0200-0093$05.00/0

condition of a low-oxygen chemical potential. The internal oxidation of metals in a helium gas atmosphere is an important problem for high-temperature gas-cooled reactors, because the oxidation causes a decrease in oxidation resistance and creep-rupture strength.[1] The helium gas contains small amounts of H_2 and H_2O, whose oxygen chemical potential is so low that the internal oxidation occurs. Although the internal oxidation is very important for practical applications, its mechanism has still not been made clear.

The diffusion process of oxygen in the alloy plays an important role in determining internal oxidation. The diffusion coefficient of oxygen has been evaluated in some alloys from internal-oxidation measurements.[2-9] Especially, the diffusion coefficient of oxygen in iron alloys cannot be determined by any other method because of the strong affinity of iron for oxygen and the small solubility of oxygen. In a previous study of the internal-oxidation behavior in the γ-phase region,[8] we pointed out that the internal-oxidation technique gives the diffusion coefficient of oxygen in the internal-oxidation layer, where the oxide exists, not that in γ-iron, and we evaluated the diffusion coefficient of oxygen, D_O, in γ-iron, In the α (δ)-phase region Swisher and Turkdogan[7] have determined the diffusion coefficient in the oxidation layer. However, D_O in α-iron has not been reported yet.

The purpose of the present study is to investigate the internal-oxidation behavior of Fe-Al alloys in the α-phase region in detail and to discuss the oxidation kinetics. The diffusion coefficient of oxygen in α-iron has also been determined with particular attention to the effect of the oxide in the oxidation layer. For this purpose the oxide formed in the oxidation layer was carefully analyzed, and the oxygen concentration at the specimen surface was determined on the basis of thermodynamics.

MATERIALS AND EXPERIMENTAL PROCEDURE

Fe-0.69, 0.158, and 0.274 wt% Al alloys were prepared by vacuum melting and swaging. Their chemical compositions are listed in Table I. Specimens of $5 \times 5 \times 4$ mm were cut and annealed in a vacuum, yielding a

Table I. Chemical Compositions of the Alloys Used.

Alloy	Al	C	Si	Mn	P	S
Fe-0.069 wt% Al	0.069	0.0030	0.011	0.006	0.004	0.004
Fe-0.158 wt% Al	0.158	0.0029	0.011	0.017	0.005	0.009
Fe-0.274 wt% Al	0.274	0.0024	0.011	0.007	0.005	0.007

grain diameter of about 85 μm. After being mechanically polished, the specimens were internally oxidized at 1023, 1073, and 1123 K. The temperature was controlled within ±2 K during oxidation. The internal oxidation was made by the method of Rhines et al.[10] using a powder mixture composed of 1 part iron, 1 part Fe_2O_3, and 1 part Al_2O_3 powders. Al_2O_3 powders were used to separate the specimen from the mixture easily. Each oxidized specimen was carefully cut into halves exactly parallel to one face of the specimen. The surface of the specimen was polished with diamond paste and then etched by 3% nital. The thickness of the internal oxidation layer was measured by an optical microscope with a micrometer stage.

The oxide formed in oxidized specimens was extracted by a bromine-alcohol method. The extracted oxide was subsequently examined by X-ray diffraction and chemical analysis in order to determine the identity and composition of the oxide.

The concentration profile of aluminum in the oxidized specimens was studied by an electron probe microanalyzer, EMPA (Hitachi X-650 type). The operating conditions of EPMA were as follows: accelerating voltage, 20 kV; specimen current, 0.012 μA; take-off angle of radiation, 38° (0.66 rad). The three alloys without oxidation treatment as well as pure iron, whose aluminum content was less than 0.001 wt%, were used as the standard specimens. Here, the relative X-ray intensity was found to be proportional to the aluminum concentration.

EXPERIMENTAL RESULTS

Internal-Oxidation Layer

A typical microstructure of Fe–0.158 wt% Al alloy internally oxidized at 1073 K for 172.8 ks is shown in Fig. 1, where S, F, and ξ indicate the specimen surface, the internal-oxidation front, and the thickness of the internal-oxidation layer, respectively. The oxidation front advances parallel to the specimen surface. A similar microstructure has been observed in Fe–Si alloys in the γ-phase region.[8] This type of internal-oxidation layer is normal according to the classification of the oxidation layers formed in iron alloys.[8]

Rate Constant for Penetration of the Internal-Oxidation Front

Figure 2 shows the square of the thickness, ξ, of the internal-oxidation layer as a function of oxidation time, t, for Fe–Al alloys oxidized at 1123 K. ξ^2 is proportional to t at each temperature. Thus, we have a parabolic rate law:

$$\xi^2 = K_p t \tag{1}$$

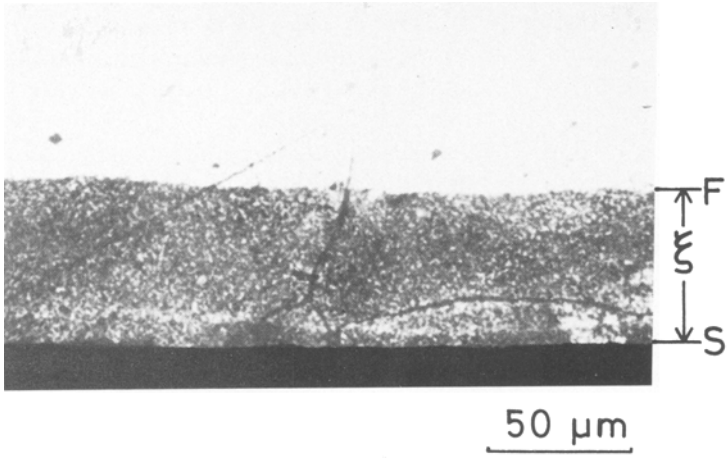

Fig. 1. A typical microstructure of an Fe–0.158 wt% Al alloy internally oxidized at 1073 K for 172.8 ks. *S*, *F*, and ξ indicate the specimen surface, the oxidation front, and the thickness of the internal-oxidation layer, respectively.

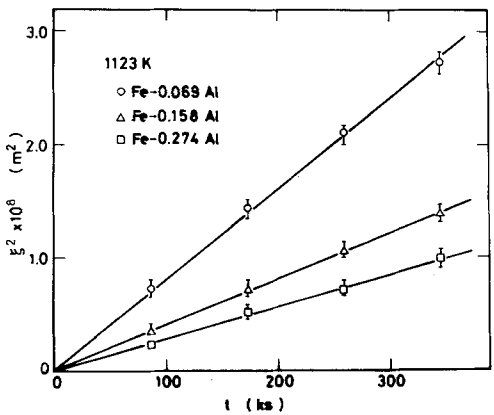

Fig. 2. The square of the thickness of the internal-oxidation layer as a function of the oxidation time in Fe–Al alloys internally oxidized at 1123 K.

where K_p is the rate constant for penetration of the oxidation front. At a constant temperature, K_p decreases as the aluminum content increases.

The temperature dependence of K_p is shown in Fig. 3. One easily sees that K_p can be expressed as

$$K_p = K_p^* \exp\left(-\frac{Q_K}{RT}\right) \tag{2}$$

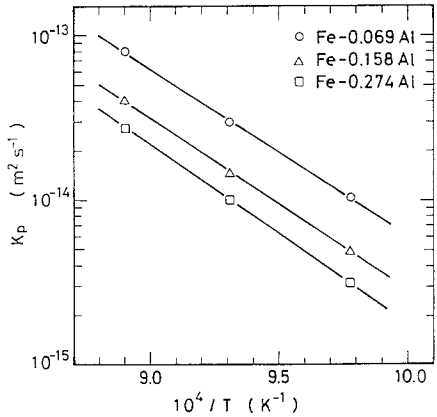

Fig. 3. Temperature dependence of the rate constant, K_p, for penetration of the internal-oxidation front.

Table II. Values of the Preexponential Factor K_p^*, and the Activation Energy, Q_K, for Penetration of the Internal-Oxidation Front in Fe-Al Alloys

Alloy	Preexponential factor, K_p^* ($m^2 \cdot s^{-1}$)	Activation energy for penetration, Q_K ($kJ \cdot mol^{-1}$)
Fe-0.069 wt% Al	9.88×10^{-5}	195 ± 5
Fe-0.158 wt% Al	8.99×10^{-5}	201 ± 4
Fe-0.274 wt% Al	1.33×10^{-4}	208 ± 3

where K_p^* is a constant, Q_K the activation energy for penetration of the internal-oxidation front, T the oxidation temperature, and R the gas constant. The estimated values of K_p^* and Q_K are listed in Table II.

Oxide and Concentration Profile of Aluminum

To determine the oxide formed in the oxidation layer, the oxide was extracted from the oxidation layer and studied by X-ray diffraction. $FeAl_2O_4$ (hercynite) was detected, but not Al_2O_3.

Figure 4 shows the concentration profile of aluminum in the Fe-0.274 wt% Al alloy oxidized at 1123 K. In the unoxidized region the aluminum concentration gradually increases as the distance from the oxidation front increases. This suggests that aluminum diffuses into the internal-oxidation layer from the bulk alloy, resulting in the increase in the aluminum

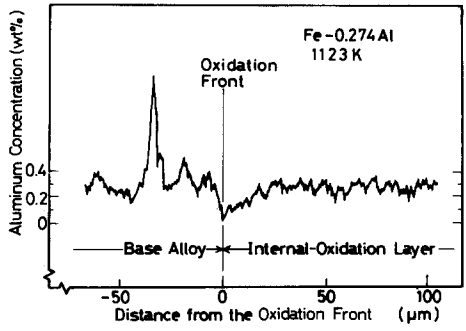

Fig. 4. Concentration profile of aluminum in an Fe-0.274 wt% Al alloy internally oxidized at 1123 K.

concentration in the oxidation layer. Such aluminum diffusion is called the counterdiffusion of aluminum. Thus, the concentration of aluminum present as an oxide in the oxidation layer is higher than its original value.

DISCUSSION

Internal-Oxidation Kinetics

The kinetics of internal oxidation, either with or without an external-oxidation layer, have been discussed theoretically by several investigators.[11-13] Oxidation where only the internal-oxidation layer is formed is discussed in the present study. We assume that the oxidation reaction takes place completely and rapidly only at the oxidation front and that the solubility product of the oxide is very low, giving rise to a negligible concentration of dissolved aluminum at the oxidation front.

A dimensionless parameter, γ, is defined by the following equation:[11]

$$\gamma = \frac{\xi}{2(D_O^{IO} t)^{1/2}} \tag{3}$$

Here, D_O^{IO} is the diffusion coefficient of oxygen in the internal-oxidation layer, in which the oxide particles are dispersed. D_O^{IO} must be different from the diffusion coefficient of oxygen in the matrix metal. If

$$\gamma \ll 1 \tag{4}$$

the rate equation for internal oxidation is given by

$$\xi^2 = \frac{2N_O^S D_O^{IO}}{\nu N_B^0} F(z) t \tag{5}$$

where

$$F(z) = \pi^{1/2} z \exp(z^2) \operatorname{erfc}(z) \tag{6}$$

and

$$z = \frac{\xi}{2(D_B t)^{1/2}} \tag{7}$$

Here, N_O^S is the concentration of dissolved oxygen at the specimen surface, and N_B^0 is the original concentration of the alloying element, B, in the alloy. ν is the atom ratio of oxygen to B in the oxide and D_B the diffusion coefficient of B in the bulk alloy.

In a limiting case where z is much larger than unity, $F(z)$ can be approximated to unity. This indicates that the outward diffusion, called the counterdiffusion, of B from the bulk alloy to the oxidation front is small compared to the inward diffusion of oxygen from the specimen surface to the front, so that enrichment of B in the oxidation layer is neglected. This condition is satisfied in the internal oxidation in some alloys.[2-4] In general cases where $F(z)$ is smaller than unity, the alloying element is enriched in the oxidation layer due to the counterdiffusion of B. The enrichment of the alloying element has been reported in some alloys.[5,8,9,12] The enrichment factor, β, is defined as

$$\beta = \frac{1}{F(z)} \tag{8}$$

Then the concentration of B, N_B^{IO}, in the internal-oxidation layer can be evaluated as

$$N_B^{IO} = \beta N_B^0 \tag{9}$$

For alloys with known D_B, β and N_B^{IO} can be obtained using Eqs. (6)-(9).

Oxide Formed in the Internal-Oxidation Layer

The oxide formed in the oxidation layer of the present alloys is $FeAl_2O_4$ as described in the previous section. In stoichiometric $FeAl_2O_4$, the atom ratio of oxygen to aluminum, ν, is 2.0. Hepworth *et al.*[6] have indicated that ν is 3.0 in the Fe-0.1 wt% Al alloy internally oxidized at 1069 K and that the high value of ν can be ascribed to some magnetite dissolved into $FeAl_2O_4$. On the other hand, Swisher and Turkdogan[7] have reported that the oxides are Al_2O_3 and $FeAl_2O_4$ at 1723 K, giving ν of 1.5-1.9, while the oxide is $FeAl_2O_4$ at 973 K.

In order to determine ν in the present alloys, the atom ratio of aluminum to iron, χ, in the oxide extracted from the oxidation layer was studied by

chemical analysis. A stoichiometric $FeAl_2O_4$ indicates $\chi = 2.0$. If the oxides are $FeAl_2O_4$ and Al_2O_3, χ would be higher than 2.0. $FeAl_2O_4$ containing some magnetite may give χ smaller than 2.0. The measured value of χ was 1.96 ± 0.05 in the Fe-0.158 wt% Al alloy oxidized at 1073 K, implying that the oxide formed in the oxidation layer of the present alloy is stoichiometric $FeAl_2O_4$ and ν is 2.0.

The enrichment of aluminum in the oxidation layer occurs in the present alloys as shown in Fig. 4. We calculated N_{Al}^{IO} with Eqs. (6)-(9). By combining Eqs. (1) and (7) we have

$$z = \frac{1}{2}\left(\frac{K_p}{D_{Al}}\right)^{1/2} \tag{10}$$

In the present study, the following data[14] on D_{Al} were used:

$$D_{Al} = (5.15^{+5.44}_{-2.64} \times 10^{-4}) \exp\left[-\frac{245.8 \pm 7.6 \text{ (kJ mol}^{-1})}{RT}\right] \text{m}^2 \text{ s}^{-1}$$

The obtained values of z, $F(z)$, and β are listed in Table III, where β is slightly higher than unity. To check the estimated values of β, the aluminum concentration in the oxidation layer was determined by both EPMA and chemical analyses. In the EPMA analysis it was determined by a graphical integration of the concentration profile of aluminum in the unoxidized region near the oxidation front. In the chemical analysis the concentration of aluminum, which was present as an oxide, in the oxidation layer was studied. The measured values of β through EPMA and chemical analyses are 1.10 ± 0.05 and 1.09 ± 0.02 for the Fe-0.274 wt% Al alloy oxidized at 1123 K, respectively. These values are in good agreement with the calculated

Table III. Values of z, β, and γ Given by Equations (10), (8), and (13), Respectively

Alloy	T (K)	z	β	γ
Fe-0.069 wt% Al	1123	3.26	1.04	3.04×10^{-2}
	1073	3.61	1.04	2.35×10^{-2}
	1023	4.23	1.03	1.78×10^{-2}
Fe-0.158 wt% Al	1123	2.31	1.08	1.98×10^{-2}
	1073	2.54	1.07	1.53×10^{-2}
	1023	2.92	1.05	1.16×10^{-2}
Fe-0.274 wt% Al	1123	1.91	1.11	1.48×10^{-2}
	1073	2.13	1.09	1.15×10^{-2}
	1023	2.33	1.08	8.71×10^{-3}

Table IV. Oxygen Concentration, N_O^S, at the Specimen Surface

Temperature (K)	1123	1073	1023
Oxygen concentration N_O^S (mole fraction)	5.51×10^{-6}	3.28×10^{-6}	1.85×10^{-6}

value of 1.11 shown in Table III. The results indicate that the counter-diffusion of aluminum is not negligible, and β in Table III is correct in the present alloys.

Oxygen Concentration at the Specimen Surface

The determination of the oxygen concentration, N_O^S, at the specimen surface is required to discuss the kinetics of the internal oxidation. Unfortunately, N_O^S in iron alloys internally oxidized in the α-phase region using a powder mixture of iron and its oxide has not yet been measured directly. We have pointed out elsewhere that N_O^S in the internal oxidation of some iron alloys is controlled by the reaction in equilibrium with Fe and FeO, even in the case of oxidation using a mixture of Fe and Fe_2O_3 powders.[9] N_O^S has been evaluated on the basis of thermodynamic data for both this reaction[15] and the solution of oxygen in α-iron.[7] Moreover, the temperature dependence of N_O^S has also been shown as

$$N_O^S = 0.381 \exp\left[-\frac{104\ (\text{kJ mol}^{-1})}{RT}\right] \tag{11}$$

The estimated values of N_O^S are given in Table IV.

Diffusion Coefficient of Oxygen in the Internal-Oxidation Layer

The diffusion coefficient of oxygen, D_O^{IO}, in the internal-oxidation layer was calculated from Eqs. (1) and (5) by using K_p, ν, $F(z)$, and N_O^S. D_O^{IO} should be distinguished from the diffusion coefficient of oxygen in α-iron, because D_O^{IO} includes the effect of the oxide in the oxidation layer. The temperature dependence of D_O^{IO} is shown in Fig. 5. For each alloy, D_O^{IO} can be expressed as

$$D_O^{IO} = A^{IO} \exp\left(\frac{-Q_O^{IO}}{RT}\right) \tag{12}$$

where A^{IO} is the frequency factor and Q_O^{IO} the activation energy for diffusion of oxygen in the oxidation layer. Table V shows the estimated values of A^{IO} and Q_O^{IO}.

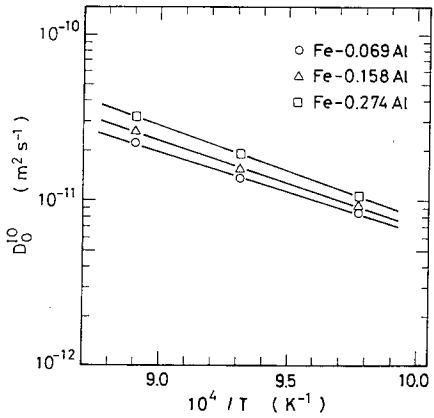

Fig. 5. Temperature dependence of the diffusion coefficient of oxygen in the internal-oxidation layer of Fe-Al alloys.

Table V. Values of the Frequency Factor, A^{IO}, and the Activation Energy, Q_O^{IO}, for Diffusion of Oxygen in the Internal-Oxidation Layer of Fe-Al Alloys

Alloy	Frequency factor, A^{IO} ($m^2 \cdot s^{-1}$)	Activation energy, Q^{IO} ($kJ \cdot mol^{-1}$)
Fe-0.069 wt% Al	4.10×10^{-7}	92.0 ± 4.3
Fe-0.158 wt% Al	1.09×10^{-6}	99.5 ± 3.7
Fe-0.274 wt% Al	2.64×10^{-6}	105 ± 3

By combining Eqs. (1) and (3), we have a dimensionless parameter, γ, as:

$$\gamma = \frac{1}{2}\left(\frac{K_p}{D_O^{IO}}\right)^{1/2} \tag{13}$$

The calculated values of γ are listed in Table III. Since γ is much smaller than unity in all of the cases, Eq. (5) is generally valid for the rate equation for the internal oxidation of the present alloys.

Figure 6 shows the effect of the volume fraction of the oxide, f^{IO}, in the oxidation layer on D_O^{IO}. f^{IO} was calculated from N_{Al}^{IO} determined using Eq. (9) and β listed in Table III. As can be seen, f^{IO} is linear in D_O^{IO} at each oxidation temperature and may be given by

$$D_O^{IO} = D_O + bf^{IO} \tag{14}$$

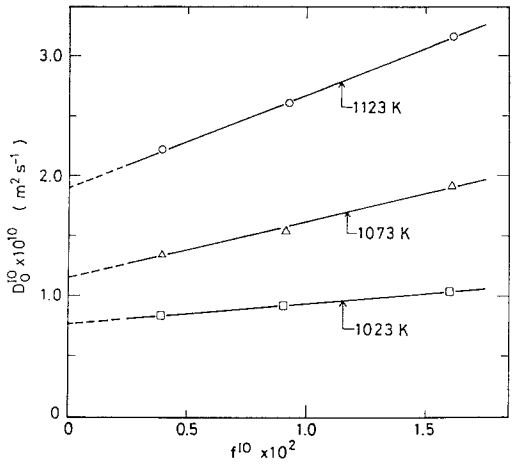

Fig. 6. The diffusion coefficient of oxygen in the internal-oxidation layer as a function of volume fraction of the oxide.

where D_O and b are constants. Similar linearity has been reported in Fe-Si[8] and Fe-Al[9] alloys in the γ-phase region as well as Ni-Cr and Ni-Al alloys.[4] The reason for the observed dependence of D_O^{IO} on f^{IO} has been shown in the previous study.[8]

Diffusion Coefficient of Oxygen in α-Iron

D_O in Eq. (14) indicates the diffusion coefficient of oxygen in the matrix metal, α-iron, in which the effect of the oxide particles is neglected. D_O was determined by an extrapolation of D_O^{IO} to $f^{IO} = 0$. The obtained temperature dependence of D_O is shown in Fig. 7. Then, D_O can be expressed as

$$D_O = (1.79^{+1.76}_{-0.89}) \times 10^{-7} \exp\left[-\frac{85.7 \pm 6.1 \text{ (kJ mol}^{-1})}{RT} \right] \text{m}^2 \text{ s}^{-1}$$

For comparison the diffusion coefficient of nitrogen, D_N, in α-iron[16] is also shown in Fig. 7, where D_O is smaller than D_N. However, the activation energy for diffusion of oxygen is in good agreement with that for diffusion of nitrogen (79.1 kJ mol^{-1}).

CONCLUSIONS

Internal-oxidation measurements of Fe–0.069, 0.158, and 0.274 wt% Al alloys were made in the α-phase region to determine the kinetics and

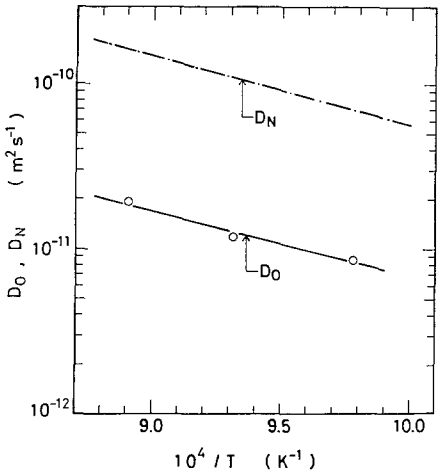

Fig. 7. Temperature dependence of the diffusion coefficient of oxygen, D_O, in the present study and that of nitrogen, D_N,[16] in α-iron.

to measure the diffusion coefficient of oxygen in α-iron. The results are summarized as follows.

1. The internal-oxidation front moves parallel to the specimen surface. The internal-oxidation process in Fe-Al alloys follows a parabolic rate law. This fact suggests that the internal oxidation is controlled by a diffusion process of oxygen in the alloys.

2. The oxide formed in the oxidation layer is a stoichiometric hercynite, $FeAl_2O_4$, having an atom ratio of oxygen to aluminum of 2.0.

3. A small enrichment of aluminum was found in the oxidation layer, which is attributable to the counterdiffusion of aluminum. The aluminum concentration in the oxidation layer calculated from the diffusion coefficient of aluminum agrees with those determined by both EPMA and chemical analyses.

4. The oxygen concentration at the specimen surface was calculated using the thermodynamic data for the reaction in equilibrium with Fe and FeO and the solution of oxygen in α-iron.

5. The diffusion coefficient of oxygen, D_O^{IO}, in the oxidation layer was evaluated from the rate equation for internal oxidation. D_O^{IO} measured is proportional to the volume fraction of the oxide, f^{IO}, in the oxidation layer.

6. The diffusion coefficient of oxygen, D_O, in α-iron was determined by extrapolating D_O^{IO} to $f^{IO}=0$. D_O is given by

$$D_O = (1.79^{+1.76}_{-0.89}) \times 10^{-7} \exp\left[-\frac{85.7 \pm 6.1 \text{ (kJ mol}^{-1})}{RT} \right] \text{m}^2 \text{ s}^{-1}$$

ACKNOWLEDGMENTS

The authors wish to express their indebtedness to Professor Z. Asaki and Dr. Y. Ueda for their helpful suggestions, K. Kimura for the X-ray diffraction work, T. Unezaki for the EPMA work, and N. Inoyama and T. Kitamura for the chemical analysis of the specimens. Special thanks are also due to Professor Y. Nakamura for his encouragement in carrying out this research. Grateful acknowledgment is also made to Nippon Kokan K. K. for supplying the alloys used.

REFERENCES

1. T. Kondo, *Bull. Japan Inst. Metals* **17**, 274 (1978).
2. J. E. Verfurth and R. A. Rapp, *Trans. AIME* **230**, 1310 (1964).
3. S. Goto, K. Nomaki, and S. Koda, *J. Japan Inst. Metals* **31**, 600 (1967).
4. S. Goto and S. Koda, *J. Japan Inst. Metals* **34**, 319 (1970).
5. K. Bohnenkamp and H. J. Engell, *Arch. Eisenhüttenw.* **35**, 1011 (1964).
6. M. T. Hepworth, R. P. Smith, and E. T. Turkdogan, *Trans. AIME* **236**, 1278 (1966).
7. J. H. Swisher and E. T. Turkdogan, *Trans. AIME* **239**, 426 (1967).
8. J. Takada, K. Kashiwagi, and M. Adachi, *J. Mat. Sci.* **19**, 3451 (1984).
9. J. Takada, Doctoral Dissertation, Kyoto University (1982).
10. F. R. Rhines, W. A. Johnson, and W. A. Anderson, *Trans. AIME* **147**, 205 (1942).
11. C. Wagner, *Z. Elektrochem.* **63**, 772 (1959).
12. F. Maak, *Z. Metallkde* **52**, 545 (1961).
13. J. Pötschke, P. M. Mathew, and M. G. Frohberg, *Z. Metallkde* **61**, 152 (1970).
14. H. Oikawa, *Tetsu-to-Hagane* **68**, 1489 (1982).
15. F. D. Richardson and J. H. E. Jeffes, *J. Iron Steel Inst.* **160**, 261 (1948).
16. P. Grieveson and E. T. Turkdogan, *Trans. AIME* **230**, 1604 (1964).